

Article

# Sampling and analysis of low molecular weight volatile metabolites in cellular headspace and mouse breath

Theo Issitt <sup>1,2</sup>, Sean T Sweeney <sup>1,2</sup>, William J Brackenbury <sup>1,2</sup> and Kelly Redeker <sup>1,\*</sup><sup>1</sup> Department of Biology and York Biomedical Research Institute, University of York, York YO10 5DD, United Kingdom<sup>2</sup> York Biomedical Research Institute, University of York, York YO10 5DD, United Kingdom

\* Correspondence: kelly.redeker@york.ac.uk

**Abstract:** Volatile compounds, abundant in breath, can be used to accurately diagnose and monitor a range of medical conditions. This offers a non-invasive, low-cost approach with screening applications; however, uptake of this diagnostic approach has been limited by conflicting published outcomes. Most published reports rely on large scale screening of the public, at single time points and without reference to ambient air. Here, we present a novel approach to volatile sampling from cellular headspace and mouse breath that incorporates multi-time point analysis and ambient air subtraction revealing compound flux as an effective proxy of active metabolism. This approach to investigating breath volatiles offers a new avenue for disease biomarker discovery and diagnosis. Using gas chromatography mass spectrometry (GC/MS), we focus on low molecular weight, metabolic substrate/by-product compounds and demonstrate that this non-invasive technique is sensitive (reproducible at ~1 µg cellular protein, or ~500,000 cells) and capable of precisely determining cell type, status and treatment. Isolated cellular models represent components of larger mammalian systems and we show that stress- and pathology-indicative compounds are detectable in mice, supporting further investigation using this methodology as a tool to identify volatile targets in human patients.

**Keywords:** Volatile organic compound; VOC; headspace; breath; breath biomarker; volatile metabolite; breath diagnosis

## 1. Introduction

Volatile Organic Compounds (VOCs) are small, carbon containing compounds that are found at least partially in the gaseous state at standard temperature and pressure. The human 'volatilome' describes the VOCs that are produced and metabolised within the human body [1]. These compounds provide valuable insights into metabolic processes and can be detected from the breath, skin, urine, faeces and saliva [1,2], providing an opportunity to diagnose and monitor treatment as well as measure bodily functions.

A large amount of research has been conducted upon human breath with a range of VOCs linked to disease [3]. However, In the field of breath and 'smell' diagnostics, more human research (e.g. - sampling individually and directly from breath) has thus far been conducted than research that tests volatile outcomes from preclinical, pathogenically representative, cellular models, limiting mechanistic understanding of VOC metabolism. There is a paucity of published research linking cellular processes and VOC metabolisms to identify diagnostically powerful and translatable VOC biomarkers of cellular and disease processes [3]. We focus here upon breath as it provides insights into systemic, internal bodily processes via diffusion between the lungs and blood.

Many methodological approaches for breath VOC collection have been described [4–7] and some metabolic processes have been linked to the volatilome, such as reactive oxygen species production of aldehydes and alkanes [1,8,9] and microbial function linked to sulphur compounds like dimethyl sulphide [3,10]. Diagnostic applications of VOCs remain limited in the clinic, in part due to conflicting and confounding results [3].

Useful VOC biomarkers should be descriptive of a condition while overcoming environmental, individual and methodological variabilities. Reported breath VOC variability accrues from individual comorbidities and variations in analytical and collection methods, leading to reduced sensitivity and lack of recognition of potentially useful biomarker compounds. Commonly used methodological approaches also rely on single time point sampling and do not take into account the ambient volatile environment, allowing environmental variability to influence and reduce reported outcome precision [3,11,12], relying instead upon substantial deviations from the norm and reducing the utility of breath volatiles through loss of information. New approaches and perspectives are therefore needed to contextualise the valuable research done so far and to identify robust volatile biomarkers to provide fast, non-invasive, low-cost diagnostics.

Metabolism of VOCs, defined here as flux (reported in grams compound per gram organism weight per time, i.e. - g g<sup>-1</sup> s<sup>-1</sup>), considers both release and consumption. Production of compounds can be an expression of metabolic products, for example; acetone release in the breath from alterations in metabolism [13] and carbon dioxide release from glucose metabolism. Emissions of VOCs may also be caused by release from saturated tissues, such as muscular release of isoprene in human breath during exercise [14]. Consumption of VOCs can also be observed through active metabolism, such as with CYP450 enzymes in the human liver [15] or consumption of oxygen. Quantifying and understanding healthy human metabolism and its impact on VOCs is a developing field and is necessary to define population variability and compound-specific standard ranges in human breath.

Uptake of compounds is not reported as often as release [3] and so volatile 'sinks', the use of VOCs by cells as substrates, may be overlooked, as a result of collection methodology and analytical focus using non targeted gas chromatography mass spectrometry techniques. Non-targeted approaches primarily detect relatively concentrated material (ppbv) whereas targeted approaches are generally capable of quantifying at much lower concentrations (pptv).

In the case of disease, understanding systemic uptake/release is critical in development of biomarkers for clinical application. Disease metabolism outcomes depend upon compound reactivity, transportation time spent within active metabolic regions or saturated tissues, and active metabolic by-products and interactions with the disease pathology [3]. Alterations in VOC flux stem from cellular environmental changes which influence metabolic response, either as a result of dysfunction or as the result of normal processes, such as exercise. Identification and separation of these processes in the volatilome is challenging because many cellular processes, dysfunctional or otherwise, produce similar changes in environmental and physiological state. For example, a shift towards glycolysis in cancer [16,17] or mitochondrial dysfunction [18], may result in similar global/tissue alterations in pH and reactive oxygen species, producing VOCs associated with this change. Breath volatiles can also be seen to change as a result of normal metabolisms, such as with fasting and eating [19,20] or circadian rhythms [21]. It is therefore important to be able to identify and characterise variation in cellular type, status (disease) and response to environmental stress.

To investigate if volatile metabolism of different cell type and status (disease) can be detected, we quantified volatile signatures (12 discrete compounds via SIM) of cells derived from two tissues and disease pathologies. We further reveal how environmental and cellular changes elicit detectable alterations in the healthy cell volatilome, through treatment with chemotherapy drug, doxorubicin. These volatile metabolisms, linked to phenotype and pathophysiology, provide potential targets for diagnostic research. We demonstrate how these cellular models are applicable in mammalian analysis through quantification of mice breath volatiles, targeting the specific compounds which have shown most promise in these early analyses.

These analyses rely upon a novel, non-invasive volatile sampling method, which allows multi-time point analysis of VOC consumption and production from cellular headspace and can be used in an ethically appropriate manner with mice volatile sampling. In

this work we use targeted mass spectrometry, or 'selective-ion mode' (SIM), and multiple time points to observe VOC metabolisms.

## 2. Results

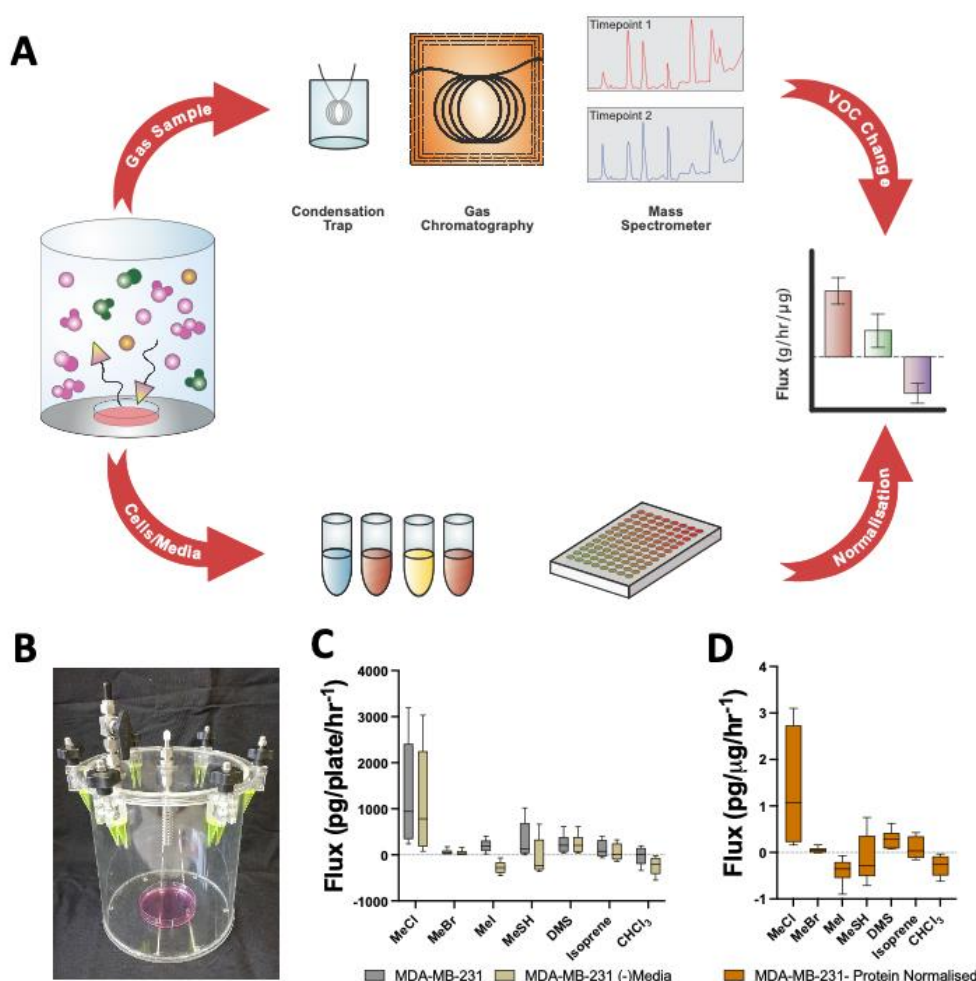


**Figure 1.** Direct volatile sampling of cellular headspace. **(A)** Schematic overview for methodological approach; headspace sampling and generation of VOC flux. **(B)** Image of collection chamber. **(C)** Selected volatile fluxes (g/hr/plate) for 10cm dishes containing DMEM media control only vs plate containing MDA-MB-231 (mean  $\pm$  SEM; n = 6). **(D)** Media subtracted and protein normalised VOC flux for MDA-MB-231 cells (mean  $\pm$  SEM; n = 6). ANOVA followed by Bonferroni post hoc test was performed; \*p < 0.05; \*\*p < 0.01; \*\*\*p < 0.001.

### 2.1. Methodological validation

The methodological approach is outlined in Figure 1a. Headspace sampling from custom chambers (Figure 1b) from multiple time points allows calculation of flux values (pg/ug/hr-1).

Headspace analysis was conducted for media only and all supplementations (DMSO and doxorubicin) controls (Figure 1, Figure S1). No significant variation was observed between DMEM, DMEM:F12 media (Figure S1 E, F, G) or with addition of DMSO (Figure S1 E, F, G). Because no variation was observed between DMEM and DMEM:F12 with DMSO addition, DMSO values represent a combination of DMEM (n = 3) and DMEM:F12 (n = 3) with DMSO addition.

Headspace above cells had appropriate media controls (average) deducted, demonstrated in Figure 1C and Figure S1A, B. This was then normalised to protein content (Figure 1D, Figure S1C, D) to give ug of compound per hour per ug of protein. This is shown

for MDA-MB-231 cells but the media subtraction process was repeated for each cell line and treatment.

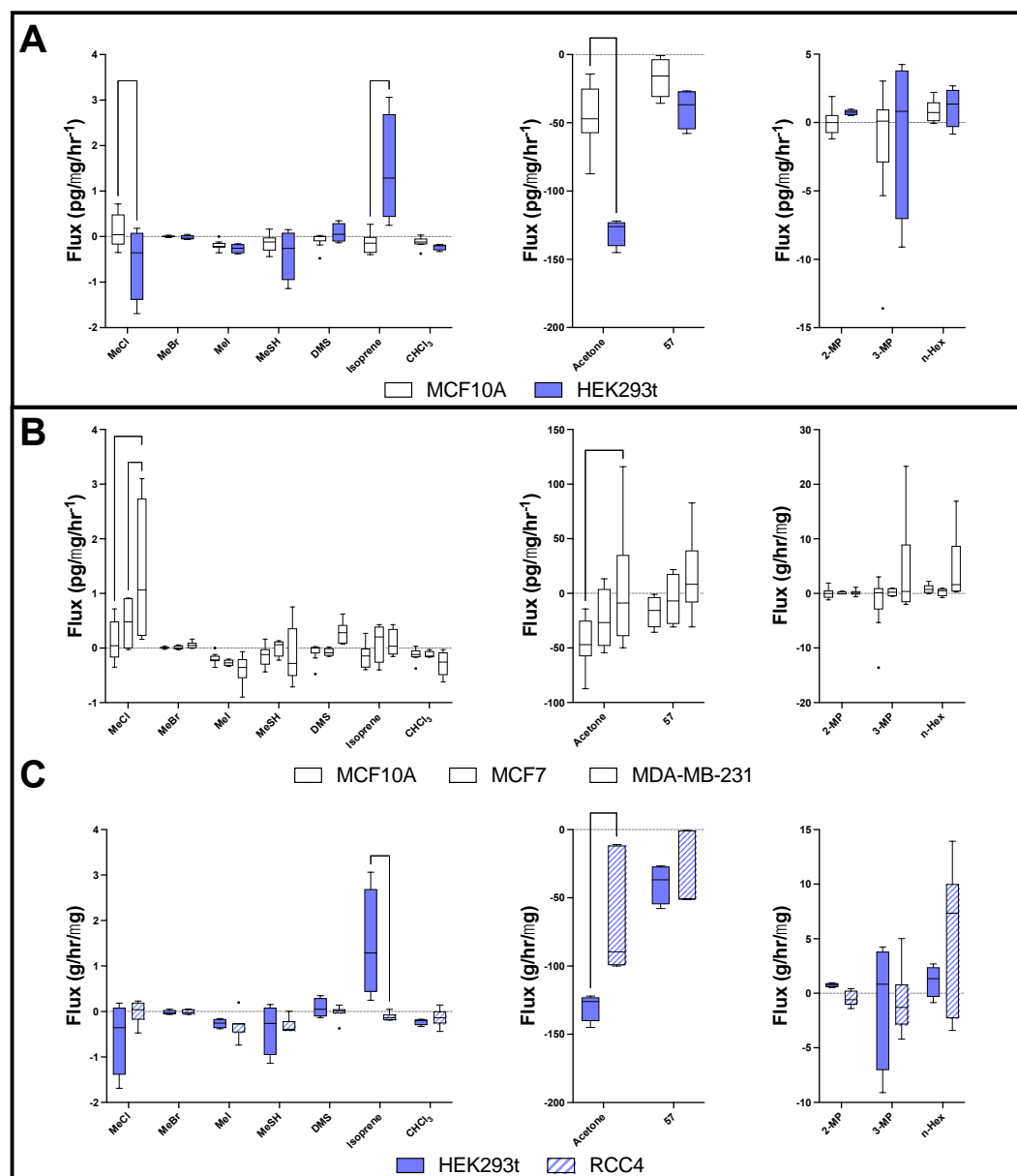


**Figure 2.** Cellular volatile profiles of breast and kidney derived cell lines. **(A)** Volatile flux (g/hr/μg) for non-cancerous derived cell lines, from breast; MCF10a and kidney; HEK293t. **(B)** Volatile flux for cancerous breast derived cell lines, MCF7 and MDA-MB-231. Volatile flux for cancerous kidney derived cell line RCC4. Media subtracted and protein normalised VOC flux for MCF10a (n = 9); MCF7 (n = 4); MDA-MB-231 cells (n = 6). CHCl<sub>3</sub> = Chloroform, DMS = Dimethyl sulfide, MeBr = Methyl bromide, MeCl = Methyl Chloride, MeI = methyl iodide, MeSH = Methanoethiol. Boxplot whiskers show median ± Tukey distribution. ANOVA followed by Bonferroni post hoc test was performed; \*p < 0.05; \*\*p < 0.01; \*\*\*p < 0.001.

## 2.2. Headspace volatile profiles differ between cell type

Comparison of cells growing at basal capacity (i.e. in fully supplemented, optimum media) within a laboratory setting revealed differences in selected volatiles in the headspace. Methyl chloride (MeCl), isoprene and acetone significantly differ between cell lines. Cancer cell lines show consistently higher levels of MeCl and acetone compared to non-cancer cell lines.

### 2.2.1. Headspace volatiles differ between breast and kidney derived cells

For non-cancer cells (Figure 2G-I); HEK293t cells show significant uptake of MeCl compared to MCF10A and significant release of isoprene (Figure 2G). HEK293T cells consumed significantly more acetone than MCF10a and M57 uptake was also increased (Figure 2H). In contrast, 2-methyl pentane (2-MP) production appears increased in HEK293T cells compared to MCF10A (Figure 2I).

### 2.2.2. Headspace volatiles differ between cancer and non-cancer breast epithelial cells

When comparing headspace samples from breast cancer MCF7 and MDA-MB-231 to those of non-cancer MCF10A cells derived from breast tissue (Figure 2A-C); MeCl levels are enhanced over MCF7 and were significantly enhanced over MDA-MB-231 cells compared with MCF10A. Methyl bromide (MeBr) and dimethyl sulfide (DMS) levels were increased over MDA-MB-231 cells compared to both MCF7 and MCF10A. MCF7 cells exhibited significantly increased production of isoprene compared to MCF10A, which exhibited isoprene uptake. MDA-MB-231 cells also reveal production of isoprene rather than consumption. Acetone uptake is reduced in MCF7 cells compared to MCF10A and MDA-MB-231 show significant changes in production of acetone, however the range is large (Figure 2B). (Figure 2E). M57 was increased in MDA-MB-231 cells compared with MCF10A.

### 2.2.3. Headspace volatiles differ between cancer and non-cancer kidney derived cells

For cells derived from kidney (Figure 2C); HEK293T cells show uptake of MeCl which is unique when compared to all other untreated cells lines. RCC4 cells show little production or consumption of MeCl. Isoprene is significantly more concentrated in the headspace of HEK293T cells compared to RCC4, which show metabolic uptake. Acetone consumption is significantly reduced in RCC4 cells compared to HEK293t (Figure 2C). RCC4 cells show some uptake of 2-MP vs HEK293T production with increased production of n-Hexane vs HEK293T (Figure 2F).

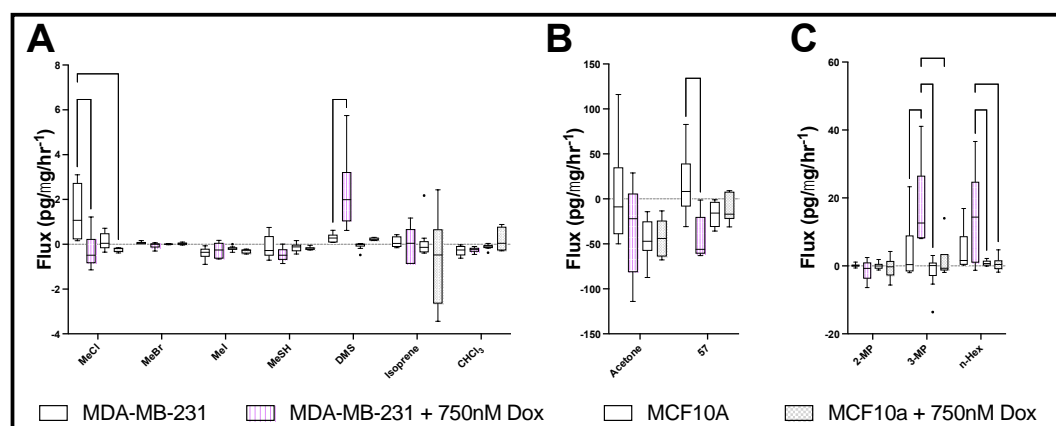


**Figure 3.** Doxorubicin induces volatile response in breast cell lines. Boxplot for select volatile organic compounds. (median  $\pm$  Tukey distribution;  $n = 6$ ). ANOVA followed by Tukey post hoc test was performed; \* $p < 0.05$ ; \*\* $p < 0.01$ ; \*\*\* $p < 0.001$ ; \*\*\*\* $p < 0.0001$ . Doxorubicin has been abbreviated to Dox

### 2.3 Doxorubicin treatment produces significant volatile headspace changes in breast derived cells

Doxorubicin treatment produced significant alterations in the volatile profile of both MCF10A and MDA-MB-231 cells as shown in Figure 3. Treatment of MDA-MB-231 with 250 nM and 750 nM revealed consistent trends with increasing concentrations (Figure S2A). For MDA-MB-231 cells, MeCl switched significantly from production to uptake with increasing concentration of doxorubicin. Methanethiol (MeSH) also showed increased uptake, while DMS was significantly increased in its release. Uptake of acetone by MDA-MB-231 cells was observed, but it was non-significant. Significant uptake by

MDA-MB-231 cells was observed for M57 with no change in MCF10A. Doxorubicin also produced significant increases in 3-methyl pentane (3-MP) and provoked n-Hexane release in MDA-MB-231 cells. MCF10A cell volatiles changed in a similar manner as MDA-MB-231 in response to doxorubicin treatment. MeCl, showed a similar shift to uptake from production, DMS production increased and chloroform ( $\text{CHCl}_3$ ) was produced.

MTT assay was performed as an indication of metabolic activity. MCF10A cells show greater metabolic activity than MDA-MB-231 cells. Treatment with doxorubicin increased metabolic activity by this assay compared to vehicle (Figure S3). Sulforhodamine B (SRB) assay revealed no significant variations for cell growth at 24 hours between treatments. At 48 hours doxorubicin treatment suppressed growth in both cell lines (Figure S3). Trypan blue exclusion revealed a non-significant reduction in cell viability at 370 and 740 nM doxorubicin for MDA-MB-231 cells and a similar but significant reduction in cell viability in MCF10a cells exposed to 740nM doxorubicin (Figure S3).

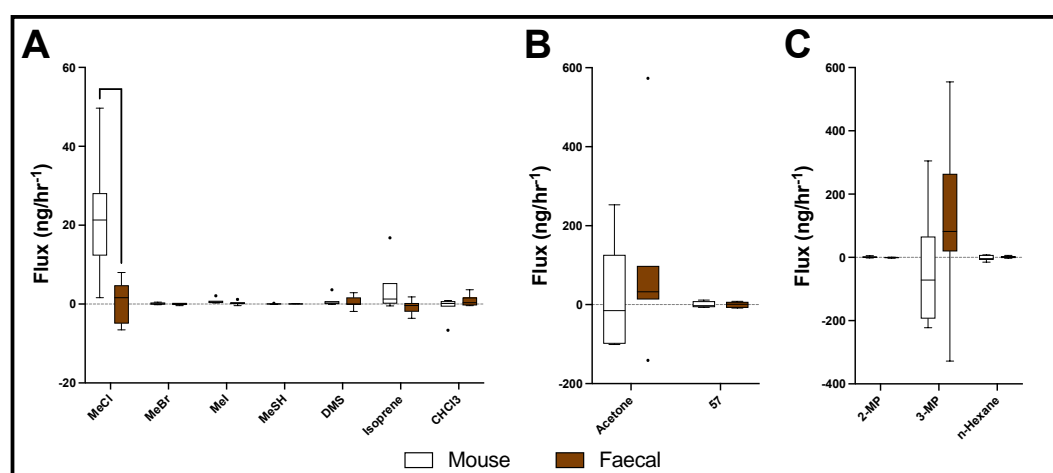


**Figure 4.** Volatile organic compounds from mouse breath and faecal material. Boxplot for select volatile organic compounds from chambers with single mice vs chambers with mice removed and faecal material. Flux in g/hr (median  $\pm$  Tukey distribution;  $n = 6$  mice across 3 separate cages). ANOVA followed by Bonferroni hoc test was performed; \*\*\*\* $p < 0.0001$

#### 2.4. Headspace volatiles from mouse breath and faecal material

Collection of breath from 9 week old female Rag2 $^{-/-}$  Il2rg $^{-/-}$  mice using the sampling chambers (Figure 1B) reveals metabolic interaction with several volatile compounds (Figure 4). Because mice were allowed to behave normally in chambers for 20 mins following 10 mins of acclimatisation, presence of mouse (in white, Figure 4) is representative of both mouse breath and faecal volatiles whereas faecal (in orange, Figure 4) indicates faecal material volatiles only.

Mice show significant positive production of MeCl compared to faecal material as well as production of isoprene (Figure 4A). 3-MP uptake by mice is significant, although the uptake is reduced by the presence of faecal matter (which generally produced 3-MP) (Figure 4C).

### 3. Discussion

This research demonstrates that volatile analysis can separate cellular models by cellular type, disease status and response to chemically induced stress. Furthermore, we have shown that representative, discrete indicator compounds are found in mouse breath and are actively produced or metabolised. A selection of these compounds, including methyl halides have also recently been reported in human breath [22]. These outcomes support further research into their potential use as biomarkers of disease.

#### 3.2. Cellular Volatiles and metabolisms

There are limited data on cellular headspace volatile concentrations, and less on volatile metabolites. Headspace volatiles for MCF10A, MCF7 and MDA-MB-231 cells have previously been investigated [23,24]. HEK293T cells have also had some limited investigation [25]. This is the first time that RCC4 cell headspace volatiles have been reported. In this work we have focused on a novel approach to describing the dynamics of 12 select VOCs, reflective of cellular metabolisms, not discovery of new volatiles using non-targeting approaches. This allows greater precision and resolution in assessment of select VOC dynamics, which is well suited to a longitudinal approach.

A further challenge in volatile breath research is the paucity of data regarding metabolic processes and alterations dependent upon compound and/or cellular type/state. For example, while chloroform exposure is well documented and the compound is broken down in the liver by CYP450 enzymes [26], its (normal) metabolic consumption and production in mammalian systems has not previously been described.

Likewise, human erythrocytes contain a glutathione-S-transferase isoenzyme that metabolises methyl halides [27,28] but this is not present in all humans [29]. Methyl halide metabolism remains unidentified and undescribed in human systems. All plants and fungi measured to date produce methyl halides but the functional reason for this metabolism remains unclear [30]. A role for active metabolism of methyl halides in mammalian systems is presented in this paper, as we have shown active production and consumption of MeCl, MeBr and MeI in varying situations. Their potential as disease biomarkers however, requires further research.

In our tested cellular systems, metabolism of MeCl is descriptive of cellular type with cancer cells exhibiting increased release relative to their healthy controls. Under treatment of doxorubicin, MeCl uptake is seen in response. Furthermore, this compound can be quantified in the breath of mice and humans. The association of methyl halides with mammalian systems has been limited, overexposure of MeCl in rats was not linked to DNA adducts where MeI and MeBr have been shown to cause systemic DNA methylation [31]. Long term exposure of MeCl at high concentrations (1000ppm) produced renal tumours in male rats and glutathione depletion [32,33].

MeSH and DMS are linked as sulphur containing compounds and are metabolites for each other, with MeSH serving as a precursor to DMS (with a methylating agent) and DMS serving as a precursor to MeSH (with a demethylating agent) [34,35]. Glutathione (GSH)-based metabolism of MeCl can result in formation of MeSH [36]. Both MeSH and DMS have been linked to bacterial processing [10,37]. Sulphur containing VOCs have been shown in human breath for a variety of diseases and processes [3]. Sulphur is also a dietary requirement [38] which suggests that diet will impact sulfur-volatile metabolism, and breath volatile concentrations, in individuals.

Isoprene and isoprenoids, as endogenous biomarkers, have been shown to be linked in patients with muscular dystrophy and are outputs of the mevalonate pathway [39]. Monitoring their levels may be important in a variety of diseases, such as cancer, as isoprenoids have been shown to be important compounds in tumour biology [40]. However, large variability between individuals, as demonstrated here and in a recent review [3] show that this volatile, while the most abundant VOC in human breath, is a challenging biomarker for individual/cohort diagnoses. Longitudinal and metabolic approaches, like those described here may prove able to utilise biomarkers with high variability between individuals but further research is required.

Alkanes have been associated with oxidative stress and reactive oxygen species induced lipid peroxidation, linked to a range of diseases [41]. 2- and 3-methyl pentane have been identified as potential markers of cancer [42,43] as has hexane [44]. Alkanes are found in the breath of patients with a range of diseases, but prevalent in cancer [3]. Methylated alkanes are also descriptive of oxidative stress in transplant rejection [1,45]. However, the interplay between methylated and straight chain alkanes is less understood and so 6 carbon alkanes were targeted here.

Of the compounds reported here, acetone is one of the most well documented, and has been identified as a volatile compound associated with altered metabolisms and the

development of ketosis [13]. Therefore its dynamics are of interest in models of cancer which show altered energy processing.

We have shown both novel VOC targets and targets previously identified in cellular headspace and breath. We propose that characterization of volatiles relative to cell type and status will allow utilization of a “breath-print” approach, where multiple volatiles indicative of specific healthy states or pathologies are combined to provide accurate and specific disease indicators. Refinement of target VOCs will increase with further research and we have recommended research frameworks previously [3].

### 3.3. Mouse Volatiles

Our approach minimises stress in animals, which directly influences the breathing profile [46,47]. This longitudinal approach also allows us to view the compounds which are being metabolised/absorbed by mice and/or their faecal matter. Like humans, these mice show release of MeCl, however it is of note that these mice are immunocompromised and their breath volatiles may differ from standard wild type mice models.

Identified active metabolisms of VOCs in mice provide targets for future disease mouse models and translates well into the breath of humans [22]. Here, we show variability over time and individual variability in mouse breath. With further research the expected and average human range for each compound may be understood, to produce standards for medical application. However, individual variability over time supports a longitudinal approach to diagnosis as direct comparisons between individuals may confound results.

### 3.4. Conclusion

Here, we have shown a new approach to VOC headspace sampling from cells in culture and mice. Using this technique, we can identify cells from different tissues and if cells from that tissue are cancerous or not. Furthermore, the response to cellular stress, from the chemotherapeutic doxorubicin, is clearly defined in the volatile profile of both MDA-MB-231 breast carcinoma cells and non-cancer MCF10A cells. However, the cancer cell line MDA-MB-231 revealed more significant alterations for MeCl, DMS, M57, 3-MP and n-Hexane. This may have implications for monitoring chemotherapeutic treatments.

Our approach to investigating volatiles considers ambient environmental compounds and the processing of those compounds by the body. Ambient compounds which are taken up by cells or the body may be active metabolic substrates or accidentally metabolised, however these reported metabolisms require further investigation. Volatile metabolisms in mammalian systems is an emerging field and the processing of environmentally available VOCs takes into consideration the use of these compounds as potential substrates or chemical interactants.

Using this approach may allow researchers to investigate volatile compounds in a new way for volatile biomarker discovery and diagnostic procedures. The compounds investigated here, including methyl halides present an opportunity to explore metabolisms as they are processed by cells and present in cellular headspace and breath. Methyl chloride is consistently enhanced in mammalian breath and cellular headspace and its significant alterations in response to cellular stress may translate well into breath. Several compounds presented here show similar promise for human diagnosis and further research is required to refine and describe the representative conditions that create specific metabolic outcomes.

## 4. Materials and Methods

### 4.1. Cell culture and treatment conditions

Breast cancer cell lines MDA-MB-231 and MCF7 and kidney derived cell lines; HEK-293T and RCC4 were grown in Dulbecco's Modified Eagle Medium (DMEM, Gibco) 25 mM glucose, supplemented with L-glutamine (4 mM) and 5% foetal bovine serum (Gibco). The non-transformed human epithelial mammary cell line MCF10A were grown in DMEM/F12 (Gibco) supplemented with 5% FBS, 4 mM L-glutamine (Gibco), 20 ng/ml EGF (Sigma), 0.5 mg/ml hydrocortisone (Sigma), 100 ng/ml cholera toxin (Sigma) and 10 µg/ml

insulin (Sigma). All cell culture media was supplemented with 0.1 mM NaI and 1 mM NaBr (to model physiological availability of iodine and bromide). All cells were grown at 37°C with 5% CO<sub>2</sub>.

To initiate the volatile collection procedure cells were trypsinized, and ~500,000 cells seeded into 8 ml complete media. Cells were then allowed to attach for 3 hours, washed with warm PBS 2x and 8ml treatment media applied. Volatile headspace sampling was performed 24 hours later.

Doxorubicin was dissolved in DMSO. Doxorubicin treatment was applied in DMEM (Gibco) 25 mM glucose, supplemented with L-glutamine (4 mM) and 5% FBS for MDA-MB-231 cells and treatment medium for MCF10A. Appropriate doxorubicin concentration was determined using MTT and SRB assays which assess metabolic activity and protein concentration as a measure of growth respectively. Concentrations for doxorubicin treatment were chosen based on no less than 25% reduction in growth of metabolic activity following 24 hours of treatment and supporting evidence in the literature of similar concentrations eliciting senescent and maintaining growth [48–50]. This was determined by SRB, MTT and trypan blue exclusion assays (Figure S3). 750 nM was chosen to induce chronic cell stress over this time period while reducing the amount of cell death.

#### 4.2. Headspace and breath sampling

##### 4.2.1. Cellular headspace sampling

Following the incubation period (24 hours), 5 ml of supernatant medium was removed and plates, with lids removed, were placed into specially constructed chambers (Figure 1B) on a platform rocker on its slowest setting. Medium was equilibrated with lab air by flushing the chamber for 20 min using a Yamitsu air pump with a flow rate of 750 ml per min. Time zero (T0) samples were taken using an evacuated 500 ml electropolished stainless steel canister (LabCommerce) through Ascarite® and Drierite® traps [51]. The chamber headspace was then isolated by closing the lid valves and the chamber itself was left on the rocker for 120 mins, at which point another air sample (T1) was collected. Cells were removed from the chamber, washed with PBS twice, and lysed in 500ul RIPA buffer (NaCl (5 M), 5 ml Tris-HCl (1 M, pH 8.0), 1 ml Nonidet P-40, 5 mL sodium deoxycholate (10 %), 1 ml SDS (10%)) with protease inhibitor (Sigma). Protein concentration of lysates were determined using Bradford assay [52]. Background (medium only) readings were taken for all medium types and treatments, cell free and DMSO (vehicle), following 24 h incubation at 37°C and 5% CO<sub>2</sub> (Figure S1). DMSO concentration was used equivalent to the highest equivalent dose of doxorubicin; 0.000008%. These readings had no significant differences (determined by ANOVA), and were therefore pooled and the averages subtracted from each individual cell reading.

##### 4.2.2. Mouse headspace sampling

Nine-week-old female Rag2<sup>-/-</sup> Il2rg<sup>-/-</sup> mice were selected for sampling. This mouse strain is an immunocompromised model. Experimental replicates were 2 mice from a cage across 3 separate litters/cages; 6 mice in total. Experiments have been reported inline with the ARRIVE guidelines.

Using tube handling methods, mice were gently placed with a cardboard tube and blue paper into the custom chambers. Flushing the chamber for 10 min using a Yamitsu air pump with a flow rate of 750 ml per min in undisturbed conditions, mice were allowed to acclimatise. T0 samples were then taken as with cellular headspace, the chambers were sealed for 20 min and T1 samples were then taken.

#### 4.3. GC-MS, calibration and peak analysis

Collected canister samples were transferred to a liquid nitrogen trap through pressure differential. Pressure change between beginning and end of “injection” was measured, allowing calculation of the moles of gas injected. Sample in the trap was then transferred, via heated helium flow, to a Restek® PoraBond Q column (25m length, 0.32mm

ID, 0.5- $\mu$ m diameter thickness) connected to a quadrupole mass spectrometer (Agilent/HP 5972 MSD). All samples here were analysed with a select ion mode (SIM) targeting the selected compound's greatest detected mass unit. All samples were run within 6 days of collection. The oven program was as follows: 35°C for 2 min, 10°C/min to 115°C, 1°C/min to 131°C and 25°C/min to 250°C with a 5 min 30 sec hold. The quadrupole, ion source, and transfer line temperatures were 280, 280, and 250°C, respectively.

Calibration was performed using standard gases (BOC Specialty Gases) and injections of various volumes, equal to different total amounts of compound. Linear regression analyses of calibration curves confirmed strong linear relationships between observed SIM peak areas and moles of gas injected for each VOC ( $r^2 > 0.9$  in all cases). For compounds not purchased as specialty gases with ppbv concentration, 1-2ml of compound in liquid phase was injected into a butyl sealed wheaton style glass vial (100ml) and allowed to equilibrate for 1 hour. 1 ml of headspace air was then removed using a gas tight syringe (Trajan, SGE) and injected into the headspace of a second 100ml butyl sealed wheaton style glass vial. This was then repeated and 1ml of the 2nd serial dilution vial was injected into the GCMS system with 29ml of lab air. This was performed for Methanethiol (MeSH (SPEXorganics)), Isoprene (Alfa Aesar), Acetone (Sigma), 2- & 3-methyl pentane and n-hexane (Thermofisher).

Nearly all reported compounds detected by the GC-MS were confirmed by matching retention times and mass-charge ( $m/z$ ) ratios with known standards. This is in addition to a compound with retention time of 27.3, with masses 57 and 43 (M57). which by relative distribution pattern was determined, tentatively, to be 2-butanone from the NIST library [53].

Concentrations were calculated using peak area. Peak area/moles injected were calculated from previously generated calibration curves. Sample VOC concentrations were then normalised to CFC-11 concentrations (240 parts-per-trillion-by-volume (ppt)). CFC-11 was used as an internal standard, per sample standard for normalisation as atmospheric concentrations of CFC-11 are globally consistent and stable [51].

To account for differences in rates of proliferation (MCF10a cells proliferate at a higher rate than both MCF7 and 231 cells), results from GCMS analysis were normalised to protein content at time of sampling per plate using a Bradford assay [52].

#### 4.4. Molecular Assays

##### 4.4.1 Sulforhodamine B assay

To determine cell growth, SRB assay was performed. The SRB assay measures cell density based on protein content [54]. Following incubation, cell monolayers were fixed with 10% (wt/vol) trichloroacetic acid (TCA) and stained for 30 min, after which the excess dye is removed by washing repeatedly with 1% (vol/vol) acetic acid. The protein-bound dye was dissolved in 10 mM Tris base solution for OD determination at 510 nm using a microplate reader [54].

##### 4.4.2. MTT assay

MDA-MB-231 and MCF10A cells were seeded onto 96 well plates at a density of 8000 cells per well. Serial dilutions across the plate were performed once cells had attached to the plate (4 hours). Cells were then placed in cell culture incubation conditions. 24 h later, 20  $\mu$ l of MTT solution was added to each well and incubated for 3 h. Medium was removed and precipitates solubilised in 100  $\mu$ l DMSO. Absorbance was then measured at 570 nm using a Clariostar Plus microplate reader (BMG Labtech, Germany).

##### 4.4.3. Trypan blue exclusion assay

Trypan blue exclusion assay was performed on MDA-MB-231 and MCF10A cells following treatment with DOX or DMSO. Following a published protocol [55], trypsinized cells were mixed with 0.4% Trypan blue solution and counted to determine the number of unstained (viable) and stained (non-viable) cells.

#### 4.5. Data analysis

Figures were arranged and statistical analyses were performed with GraphPad (Prism). Specific statistical analysis can be seen in figure legends. ANOVA with Bonferroni or Tukey post hoc analysis was performed for each data set to determine statistical significance.

#### 4.6. Ethical approval

Approval for all animal procedures was granted by the University of York Animal Welfare and Ethical Review Body. All procedures were carried out under authority of a UK Home Office Project Licence and associated Personal Licences.

**Supplementary Materials:** The following supporting information can be downloaded at: [www.mdpi.com/xxx/s1](http://www.mdpi.com/xxx/s1), Figure S1: title; Table S1: title; Video S1: title.

**Author Contributions:** Conceptualization, Theo Issitt, William J. Brackenbury and Kelly Redeker; Data curation, Theo Issitt; Formal analysis, Theo Issitt; Funding acquisition, Sean T Sweeney, William J. Brackenbury and Kelly Redeker; Investigation, Theo Issitt; Methodology, Theo Issitt and Kelly Redeker; Project administration, Theo Issitt and Sean T Sweeney; Resources, William J. Brackenbury; Visualization, Theo Issitt; Writing – original draft, Theo Issitt; Writing – review & editing, Sean T Sweeney, William J. Brackenbury and Kelly Redeker.

**Funding:** This research was funded by white rose mechanistic biology doctoral training program. Supported by the Biotechnology and Biological Science Research Council (BBSRC) BB/M011151/1.

**Acknowledgments:** The authors would like to acknowledge the support provided by Mark Bentley in the University of York department of biology workshop.

**Conflicts of Interest:** The authors declare no conflict of interest

## References

1. Amann A, Costello B de L, Miekisch W, Schubert J, Buszewski B, Pleil J, et al. The human volatilome: volatile organic compounds (VOCs) in exhaled breath, skin emanations, urine, feces and saliva. *J Breath Res.* 2014;8: 034001. doi:10.1088/1752-7155/8/3/034001
2. Drabińska N, Flynn C, Ratcliffe N, Belluomo I, Myridakis A, Gould O, et al. A literature survey of all volatiles from healthy human breath and bodily fluids: the human volatilome. *Journal of Breath Research.* 2021. p. 034001. doi:10.1088/1752-7163/abf1d0
3. Issitt T, Wiggins L, Veysey M, Sweeney S, Brackenbury W, Redeker K. Volatile compounds in human breath: critical review and meta-analysis. *J Breath Res.* 2022. doi:10.1088/1752-7163/ac5230
4. Blanchet L, Smolinska A, Baranska A, Tigheelaar E, Swertz M, Zhernakova A, et al. Factors that influence the volatile organic compound content in human breath. *J Breath Res.* 2017;11: 016013. doi:10.1088/1752-7163/aa5cc5
5. Lawal O, Ahmed WM, Nijssen TME, Goodacre R, Fowler SJ. Exhaled breath analysis: a review of “breath-taking” methods for off-line analysis. *Metabolomics.* 2017. doi:10.1007/s11306-017-1241-8
6. Bruderer T, Gaisl T, Gaugg MT, Nowak N, Streckenbach B, Müller S, et al. On-Line Analysis of Exhaled Breath Focus Review. *Chem Rev.* 2019;119: 10803–10828. doi:10.1021/acs.chemrev.9b00005
7. Hanna GB, Boshier PR, Markar SR, Romano A. Accuracy and Methodologic Challenges of Volatile Organic Compound–Based Exhaled Breath Tests for Cancer Diagnosis. *JAMA Oncology.* 2019. p. e182815. doi:10.1001/jamaoncol.2018.2815
8. Shibamoto T. Analytical methods for trace levels of reactive carbonyl compounds formed in lipid peroxidation systems. *J Pharm Biomed Anal.* 2006;41: 12–25. doi:10.1016/j.jpba.2006.01.047
9. Liu Y, Li W, Duan Y. Effect of H<sub>2</sub>O<sub>2</sub> induced oxidative stress (OS) on volatile organic compounds (VOCs) and intracellular metabolism in MCF-7 breast cancer cells. *J Breath Res.* 2019;13: 036005. doi:10.1088/1752-7163/ab14a5
10. Hanouneh IA, Zein NN, Cikach F, Dababneh L, Grove D, Alkhouri N, et al. The breathprints in patients with liver disease identify novel breath biomarkers in alcoholic hepatitis. *Clin Gastroenterol Hepatol.* 2014;12: 516–523. doi:10.1016/j.cgh.2013.08.048
11. Di Gilio A, Palmisani J, Ventrella G, Facchini L, Catino A, Varesano N, et al. Breath Analysis: Comparison among Methodological Approaches for Breath Sampling. *Molecules.* 2020;25. doi:10.3390/molecules25245823
12. Doran SLF, Romano A, Hanna GB. Optimisation of sampling parameters for standardised exhaled breath sampling. *J Breath Res.* 2017;12: 016007. doi:10.1088/1752-7163/aa8a46
13. Das S, Pal S, Mitra M. Significance of Exhaled Breath Test in Clinical Diagnosis: A Special Focus on the Detection of Diabetes Mellitus. *J Med Biol Eng.* 2016;36: 605–624. doi:10.1007/s40846-016-0164-6

14. Hori A, Suijo K, Kondo T, Hotta N. Breath isoprene excretion during rest and low-intensity cycling exercise is associated with skeletal muscle mass in healthy human subjects. *J Breath Res.* 2020;15: 016009. doi:10.1088/1752-7163/abbf39
15. O'Hara ME, Fernández Del Río R, Holt A, Pemberton P, Shah T, Whitehouse T, et al. Limonene in exhaled breath is elevated in hepatic encephalopathy. *J Breath Res.* 2016;10: 046010. doi:10.1088/1752-7155/10/4/046010
16. Feinberg T, Herbig J, Kohl I, Las G, Cancilla JC, Torrecilla JS, et al. Cancer metabolism: the volatile signature of glycolysis—in vitro model in lung cancer cells. *J Breath Res.* 2017;11: 016008. Available: <https://iopscience.iop.org/article/10.1088/1752-7163/aa51d6/pdf>
17. Sreedhar A, Zhao Y. Dysregulated metabolic enzymes and metabolic reprogramming in cancer cells. *Biomed Rep.* 2018;8: 3–10. doi:10.3892/br.2017.1022
18. Issitt T, Bosseboeuf E, De Winter N, Dufton N, Gestri G, Senatore V, et al. Neuropilin-1 Controls Endothelial Homeostasis by Regulating Mitochondrial Function and Iron-Dependent Oxidative Stress. *iScience.* 2019;11: 205–223. doi:10.1016/j.isci.2018.12.005
19. Statheropoulos M, Agapiou A, Georgiadou A. Analysis of expired air of fasting male monks at Mount Athos. *J Chromatogr B Analyt Technol Biomed Life Sci.* 2006;832: 274–279. doi:10.1016/j.jchromb.2006.01.017
20. Krilaviciute A, Leja M, Kopp-Schneider A, Barash O, Khatib S, Amal H, et al. Associations of diet and lifestyle factors with common volatile organic compounds in exhaled breath of average-risk individuals. *J Breath Res.* 2019;13: 026006. doi:10.1088/1752-7163/aaf3dc
21. Wilkinson M, Maidstone R, Loudon A, Blaikley J, White IR, Singh D, et al. Circadian rhythm of exhaled biomarkers in health and asthma. *Eur Respir J.* 2019;54. doi:10.1183/13993003.01068-2019
22. Shahi F, Forrester S, Redeker K, Chong JPJ, Barlow G. Case Report: The effect of intravenous and oral antibiotics on the gut microbiome and breath volatile organic compounds over one year. *Wellcome Open Research.* 2022;7: 50. doi:10.12688/wellcomeopenres.17450.1
23. Silva CL, Perestrelo R, Silva P, Tomás H, Câmara JS. Volatile metabolomic signature of human breast cancer cell lines. *Sci Rep.* 2017;7: 43969. doi:10.1038/srep43969
24. Lavra L, Catini A, Ulivieri A, Capuano R, Baghernajad Salehi L, Sciacchitano S, et al. Investigation of VOCs associated with different characteristics of breast cancer cells. *Sci Rep.* 2015;5: 13246. doi:10.1038/srep13246
25. Li Z, Shu J, Yang B, Xu C, Zou Y, Sun W. Evaluating the relationship between cell viability and volatile organic compound production following DMSO treatment of cultured human cells. *Pharmazie.* 2016;71: 727–732. doi:10.1691/ph.2016.6075
26. Constan AA, Sprankle CS, Peters JM, Kedderis GL, Everitt JI, Wong BA, et al. Metabolism of chloroform by cytochrome P450 2E1 is required for induction of toxicity in the liver, kidney, and nose of male mice. *Toxicol Appl Pharmacol.* 1999;160: 120–126. doi:10.1006/taap.1999.8756
27. Redford-Ellis M, Gowenlock AH. Studies on the reaction of chloromethane with human blood. *Acta Pharmacol Toxicol.* 1971;30: 36–48. doi:10.1111/j.1600-0773.1971.tb00632.x
28. Hallier E, Deutschmann S, Reichel C, Bolt HM, Peter H. A comparative investigation of the metabolism of methyl bromide and methyl iodide in human erythrocytes. *Int Arch Occup Environ Health.* 1990;62: 221–225. doi:10.1007/BF00379437
29. Peter H, Deutschmann S, Reichel C, Hallier E. Metabolism of methyl chloride by human erythrocytes. *Arch Toxicol.* 1989;63: 351–355. doi:10.1007/BF00303122
30. Manley SL. Phyto-genesis of halomethanes: A product of selection or a metabolic accident? *Biogeochemistry.* 2002;60: 163–180. doi:10.1023/A:1019859922489
31. Bolt HM, Gansewendt B. Mechanisms of carcinogenicity of methyl halides. *Crit Rev Toxicol.* 1993;23: 237–253. doi:10.3109/10408449309105011
32. A Chronic Inhalation Toxicology Study of in Rats and Mice Exposed to Methyl Chloride. Chemical Industry Institute of Toxicology; 1982. Available: <https://play.google.com/store/books/details?id=msszPwAACAAJ>
33. Hallier E, Jaeger R, Deutschmann S, Bolt HM, Peter H. Glutathione conjugation and cytochrome P-450 metabolism of methyl chloride in vitro. *Toxicol In Vitro.* 1990;4: 513–517. doi:10.1016/0887-2333(90)90109-7
34. Carrión O, Pratscher J, Curson ARJ, Williams BT, Rostant WG, Murrell JC, et al. Methanethiol-dependent dimethylsulfide production in soil environments. *ISME J.* 2017;11: 2379–2390. doi:10.1038/ismej.2017.105
35. Carrión O, Pratscher J, Richa K, Rostant WG, Farhan UI Haque M, Murrell JC, et al. Methanethiol and Dimethylsulfide Cycling in Stiffkey Saltmarsh. *Front Microbiol.* 2019;10: 1040. doi:10.3389/fmicb.2019.01040
36. Arts J, Kellert M, Pottenger L, Theuns-van Vliet J. Evaluation of developmental toxicity of Methyl Chloride (Chloromethane) in rats, mice, and rabbits. *Regul Toxicol Pharmacol.* 2019;103: 274–281. doi:10.1016/j.yrtph.2019.02.001
37. De Vincentis A, Vespasiani-Gentilucci U, Sabatini A, Antonelli-Incalzi R, Picardi A. Exhaled breath analysis in hepatology: State-of-the-art and perspectives. *World J Gastroenterol.* 2019;25: 4043–4050. doi:10.3748/wjg.v25.i30.4043
38. World Health Organisation. Energy and protein requirements. Report of a joint FAO/WHO/UNU Expert Consultation. *World Health Organ Tech Rep Ser.* 1985;724: 1–206. Available: <https://www.ncbi.nlm.nih.gov/pubmed/3937340>
39. King J, Mochalski P, Unterkofler K, Teschl G, Klieber M, Stein M, et al. Breath isoprene: muscle dystrophy patients support the concept of a pool of isoprene in the periphery of the human body. *Biochem Biophys Res Commun.* 2012;423: 526–530. doi:10.1016/j.bbrc.2012.05.159
40. Mo H, Jeter R, Bachmann A, Yount ST, Shen C-L, Yeganehjoo H. The Potential of Isoprenoids in Adjuvant Cancer Therapy to Reduce Adverse Effects of Statins. *Front Pharmacol.* 2019;9. doi:10.3389/fphar.2018.01515

41. Calenic B, Miricescu D, Greabu M, Kuznetsov AV, Troppmair J, Ruzsanyi V, et al. Oxidative stress and volatile organic compounds: interplay in pulmonary, cardio-vascular, digestive tract systems and cancer. *Open Chemistry*. 2015;13. doi:10.1515/chem-2015-0105
42. Phillips M, Cataneo RN, Cummin ARC, Gagliardi AJ, Gleeson K, Greenberg J, et al. Detection of lung cancer with volatile markers in the breath. *Chest*. 2003;123: 2115–2123. doi:10.1378/chest.123.6.2115
43. Kischkel S, Miekisch W, Sawacki A, Straker EM, Trefz P, Amann A, et al. Breath biomarkers for lung cancer detection and assessment of smoking related effects--confounding variables, influence of normalization and statistical algorithms. *Clin Chim Acta*. 2010;411: 1637–1644. doi:10.1016/j.cca.2010.06.005
44. Corradi M, Poli D, Banda I, Bonini S, Mozzoni P, Pinelli S, et al. Exhaled breath analysis in suspected cases of non-small-cell lung cancer: a cross-sectional study. *J Breath Res*. 2015;9: 027101. doi:10.1088/1752-7155/9/2/027101
45. Phillips M, Boehmer JP, Cataneo RN, Cheema T, Eisen HJ, Fallon JT, et al. Heart allograft rejection: detection with breath alkanes in low levels (the HARDBALL study). *J Heart Lung Transplant*. 2004;23: 701–708. doi:10.1016/j.healun.2003.07.017
46. Lim R, Zavou MJ, Milton P-L, Chan ST, Tan JL, Dickinson H, et al. Measuring respiratory function in mice using unrestrained whole-body plethysmography. *J Vis Exp*. 2014; e51755. doi:10.3791/51755
47. Noble DJ, Goolsby WN, Garraway SM, Martin KK, Hochman S. Slow Breathing Can Be Operantly Conditioned in the Rat and May Reduce Sensitivity to Experimental Stressors. *Front Physiol*. 2017;8: 854. doi:10.3389/fphys.2017.00854
48. Inao T, Kotani H, Iida Y, Kartika ID, Okimoto T, Tanino R, et al. Different sensitivities of senescent breast cancer cells to immune cell-mediated cytotoxicity. *Cancer Sci*. 2019;110: 2690–2699. doi:10.1111/cas.14116
49. You R, Dai J, Zhang P, Barding GA Jr, Raftery D. Dynamic Metabolic Response to Adriamycin-Induced Senescence in Breast Cancer Cells. *Metabolites*. 2018;8. doi:10.3390/metabo8040095
50. Bar-On O, Shapira M 'anit, Hershko DD. Differential effects of doxorubicin treatment on cell cycle arrest and Skp2 expression in breast cancer cells. *Anticancer Drugs*. 2007;18: 1113–1121. doi:10.1097/CAD.0b013e3282ef4571
51. Redeker KR, Davis S, Kalin RM. Isotope values of atmospheric halocarbons and hydrocarbons from Irish urban, rural, and marine locations. *J Geophys Res*. 2007;112. doi:10.1029/2006jd007784
52. Bradford MM. A rapid and sensitive method for the quantitation of microgram quantities of protein utilizing the principle of protein-dye binding. *Anal Biochem*. 1976;72: 248–254. doi:10.1006/abio.1976.9999
53. Wallace WE. Mass spectra. NIST chemistry webbook, NIST standard reference database. 2020.
54. Vichai V, Kirtikara K. Sulforhodamine B colorimetric assay for cytotoxicity screening. *Nat Protoc*. 2006;1: 1112–1116. doi:10.1038/nprot.2006.179
55. Strober W. Trypan Blue Exclusion Test of Cell Viability. *Curr Protoc Immunol*. 2015;111: A3.B.1–A3.B.3. doi:10.1002/0471142735.ima03bs111